Studies on Dangling bonds effect on coupling nature of $BiFeO_3$ multiferroic nanoparticles

B. Jaya Prakash[1a]*, & K. Srinivasa Rao[2b]
[1]Department of Physics, B.T. College, Madanapalle-517325, A.P., INDIA.
[2]Department of Physics, Govt. Degree College, Mandapeta -533308, A.P., INDIA.
[a]jpsvut@gmail.com

Key words: Coupling coefficient, Dangling bonds, RT Multiferroic materials, Chemical co-precipitation

Abstract. Room temperature multiferroic materials plays significant role for developing multifunctional devices for advances in science and technologies. Effective Utility of these materials depends on mutually control between by the ferroric orders and its coupling coefficient. Bismuth ferrite has gained significant importance due to its room temperature ferroic orders.

Study of the occurrence of Dangling bond and its impact on mechanical, chemical and its physical properties are gained much significance at nano scale. Occurrence dangling bonds generate a high local energy, influences much on lattice distortion and tilting of octahedral symmetry prevoskite Bismuth ferrite nanoparticles. Which intern influences greatly on multiferroic properties of and it's coupling nature material. Bismuth ferrites are synthesized by chemical co-precipitation method to achieve nano size particles and samples are sintered at different temperatures to study variation of coupling coefficient to optimize best coupling between ferroic orders based on dangling bond effect and free surface energy of the sample. For optimized sample, Characterizations has been carried out such as TG-DTA, XRD, HR-SEM, P-E hysteresis loop M-H hysteresis loop.

Introduction. Multifunctional materials have been emerging with several useful features in the same substance and displaying interestingly certain new phenomena. Such materials are the most important for future technological devises applications [1-3]. In generally, conventional materials, ferroic orders exhibited by different materials and are used in different applications separately [4, 5]. But existence of all ferroic orders in a material with single phase becomes scientific relevance in the present days for the development of multifunctional devises applications such as such as generation of multistate memories, spintronics, sensors and microelectronics devices [6, 7]. The uniqueness of these materials lies on possibility of simultaneous exploitation of their magnetization and electrical polarization state causes mutually tenability or controllability (coupling nature) over each other [8]. Such coupling coefficient of the multiferroic materials are may influenced by so many factors such as composition of the material, crystal structural, phase change, impurities, nature of ferroic orders, occurring of the ferroelectricity and magnetism with temperature and arise from different mechanisms, direction of occurring frroic orders, and dangling bond due to point defect, particle size sintering time, sintering temperature.

At present, gigantic effort has been made to explore the room temperature multiferroic materials in the past few years. Among the multiferroic materials, $BiFeO_3$ has gained great importance to realizing its technological applications at room temperature. In the present study, effect of dangalling bonds effect defect on coupling nature of the $BiFeO_3$ materials with different sintering temperatures has been analyzed with help of thermodynamic parameters. $BiFeO_3$ nanoparticles are prepared by co-precipitation method and its structural, magnetic, electrical are studied to understand the mutually controllability between ferroic orders [9].

Preparation of $BiFeO_3$ nanoparticles. Stoichiometric amount of Bi $(NO_3)_3$ (99.99%) AR grade (SRL chemicals) was dissolved in distilled water (100 ml) and iron nitrate (Fe $(NO_3)_3$) was dissolved in distilled water (100 ml).Then solutions of $Bi(NO_3)_3$ and $Fe(NO_3)_3$ were mixed homogenously by using a magnetic stirrer 10 hrs. Then ammonium hydroxide (NH_4OH) was added to the above solution drop by drop with a constant stirring of the above solution mixture to have the pH value > 9.5 in order to ensure upon a complete precipitation. After filtering, the precipitate was washed for several times using distilled water and precipitation was dried in an oven at 100 °C for 10 hrs to remove the moisture and the sample has been sintered at 400 °C, 450 °C, 500 °C, 550 °C, 600 °C, 650 °C, 700 °C, 750 °C and 800 °C for 5 hrs. Thus, received powders pressed into circular shaped pellets in 1cm diameter with a thickness of 1.5 mm using a hydraulic pellet making machine.

Measurements-Characterization studies. XRD patterns were recorded for the $BiFeO_3$ samples sintered at various temperatures using XRD 3003TT Seifert diffractometer with CuK_α radiation (λ=1.5406 Å) at 40 KV and 20 mA with a Si detector. The samples were scanned in the 2θ range of 20° -60° at the rate of two degrees per minute. The morphology of the $BiFeO_3$ samples was examined on a Tescan Vega-3 SBU scanning electron microscope. The elemental analysis of the synthesized powders was carried out using an EDAX attachment to the SEM system. Magnetic properties, M-H hysteresis loops were measured at 20 and 300 K by a vibration sample magnetometer. Ferroelectric hysteresis loop measurements were performed using Sawyer- Tower circuit setup at room temperature.

Results and discussion

Simultaneous measurement of TGA-DTA allows both heat flow and weight changes in a $BiFeO_3$ sample as a function of temperature in air atmosphere as shown in Fig. 1.

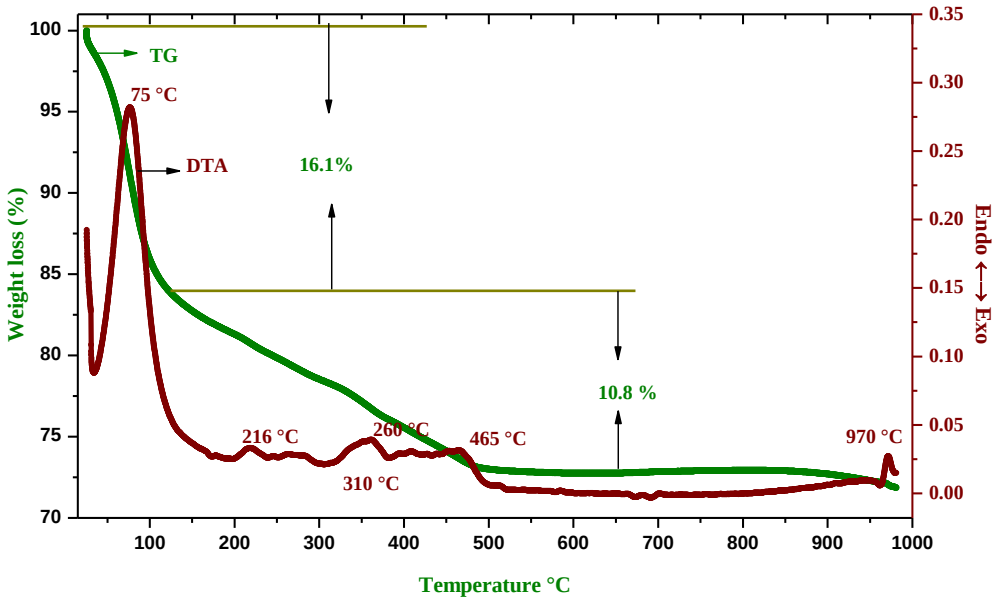

Fig.1. TG-DTA profiles of as synthesized $BiFeO_3$ nanoparticles.

TG measurement clearly shows the thermal decomposition process which in turn facilitates estimation of sample structures and compositions. The complementary information obtained allows differentiation between endothermic and exothermic events with no associated weight loss (melting and crystallization) and those involve a weight loss [10-11]. The events of changes which encountered during TG-DTA on synthesized $BiFeO_3$ nano particles are presented in Table 1. The TG profile shows the weight loss of the sample in a multi step process in the temperature range of 30 ºC -1000 ºC and the initial mass of sample is 8.023 mg. The initial and major weight loss of the sample has been taken place between 30 ºC - 100 ºC and the observed weight loss is 1.29 mg (16.1%), this weight loss corresponds

to the evaporation of water, residual solvent, combustion of organic species and decomposition of oxalate group, respectively. DTA analysis shows one broad and strong endothermic peak at 75ºC within the temperature range 30 ºC- 100 ºC. The occurrence of endothermic peaks in the temperature range, the magnitude of which depends on the synthesis method carried out. The first endothermic peak at 75ºC corresponds to the phase change of the sample from semi-solid phase to solid phase, because the starting stage of precipitation that was taken to carry out TG-DTA measurement is in the form of paste. The second weight loss has been noticed in the temperature range 100 ºC-600 ºC is equal to 0.866 mg (10.8%) due to the combustion of remaining intermediate oxalate, loss of carbonates and hydrogen, respectively. In the temperature range of 400 ºC-600 ºC, DTA curve shows an endothermic at 310 ºC and an exothermic peaks at 216 ºC, 260ºC, and 465ºC respectively. The endothermic peak at 310ºC corresponds to the release of water and combustion of organic species and may be the combustion of intermediate oxalates and loss of carbonates [12,13]. The exothermic peak at 216 ºC due to the evolution of NO_3 and 260 ºC indicates the partial crystallization process is takes place in the sample [18]. The exothermic occurred at 465ºC ordering of the perfect crystallization process [14], it also observed from XRD profiles to change from semi-crystalline structure to pure crystalline structure.

Between temperatures 600 and 1000 ºC, there is no weight loss of sample, but there is another exothermic peak at 970 ºC representing the melting point of sample. When the weight loss of the sample becomes constant that means all volatiles and impurities are removed the required sample is formed [15]. Based on the weight loss of the sample from thermo gravimetric analysis (TGA), the major weight loss of the sample is occurring between from 30 - 500 °C and above 500°C temperature weight loss appears to be small, which indicates possibility of formation of the pure $BiFeO_3$ phase.

Table 1 Details of TG-DTA profiles of $BiFeO_3$ nanoparticles

Temperature range	**TGA Profile**		**DTA Profile**	
	Sample initial weight : 8.023 mg			
	Weight loss (%)	**Weight loss (mg)**	**Exothermic**	**Endothermic**
28 ºC - 100 ºC	16.1	1.29	--	75
100 ºC-600 ºC	10.8	0.866	216,260	465
600 ºC-1000 ºC	Constant	Constant	970	--
Sample residual weight at 1000 ºC: 5.867 mg ((73.15%)				

Table 2 Details of thermodynamic parameters TG-DTA profiles of

Temperature (ºC)	Reaction	Entropy	Enthalpy (ΔH)	Gibbs Energy (ΔG)	Nature of processes
75	Endothermic	-Ve	+Ve	- Ve	Spontaneous process
216	Exothermic	+Ve	-Ve	+Ve	Non Spontaneous process
260	Exothermic	+Ve	-Ve	+Ve	Non Spontaneous process
310	Endothermic	-Ve	+Ve	- Ve	Spontaneous process
465	Endothermic	-Ve	+Ve	-Ve	Spontaneous process
970	Exothermic	+Ve	-Ve	+Ve	Non Spontaneous process

Based on the reactions exist in TG-DTA profile, Thermodynamic parameters of the prepared BiFeO3 nanoparticles are presented in Table 2. Initially, As prepared sample (semi solid), sample

having the high Helmholtz Free Energy with respect to surrounding create the mobility among atoms in addition to external heat. Further it has been reduced due to evaporation of volatile evaporation of water, residual solvent and other. During the heating of the sample, entropy of sample has been changed based on existence of thermodynamic reactions. Sample heated around at 465 ºC, Enthalpy of the sample is positive which indicates the bond energy and formation of crystal structure and it is occurred the spontaneously where Gibbs Energy is negative. .. Based on this profile, $BiFeO_3$ nanoparticles are sintered at different temperatures 500 °C, 550 °C, 600 °C 650 °C, 700°C, 750 °C and 800 °C respectively.

X-ray diffraction profiles of the $BiFeO_3$ powders sintered at different temperatures are shown in Fig.2. It is observed that, $BiFeO_3$ sample sintered at 450 °C and below is purely amorphous natured and no crystalline peaks has been observed. Because, amount of heat energy supplied at 450 °C to sample is not sufficient to form crystalline/ bonding nature between its constituent atoms. And further sample sintered at 500 °C & 550 °C, few crystalline peaks are observed with less intensity and further increasing the sintering temperature between 600 °C & 700 °C crystalline nature has been improvised with high intensity diffraction peaks (compare to sample sintered at 500 °C & 550 °C) and later the intensity of the diffraction peaks has diminished for further increase of sintering temperature between 700 °C- 800 °C indicating as it is reaching close to the melting point. XRD patterns of the sample sintered at 700 °C are in well agreement with the data of JCPDS card No: 86-1518 demonstrating the formation of $BiFeO_3$ in Rhombohedra crystal structure with lattice parameters, a =b = 5.577Å and c = 13.861Å having space group *R3c(161)* [16-19]. The average crystallite size is calculated from Scherrer's formula ($t = K\lambda / (B \cos\theta_B)$), where t is the average size of the particles, assuming particles to be spherical, K = 0.9, λ (=1.5406 Å) is the wavelength of X-ray radiation, B is the full width at half maximum of the diffracted peak and θ_B is the angle of diffraction [20-21].

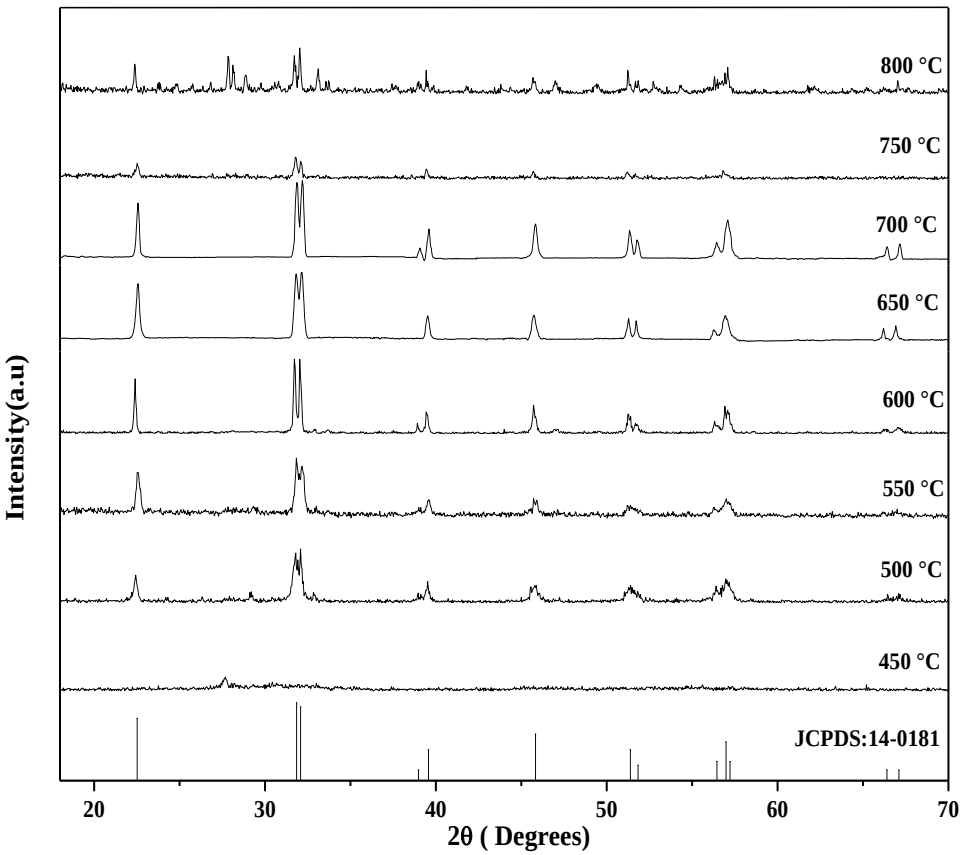

Fig.2. XRD profiles of as $BiFeO_3$ nanoparticles sintered at different temperature

The estimated average crystallite sizes of the $BiFeO_3$ samples prepared at different sintering temperatures are tabulated in Table.1. The lattice strain in nanoparticles increases with an increase in particle size during sintering of the sample.

Table.3 the average crystallite sizes of $BiFeO_3$ nanoparticles

Sintering temperature ($^{\circ}C$)	Diffraction peak position ($2\theta^{0}$)	FWHM B (radians)	Average crystallite size (nm)
500	31.6	0.272	34
600	31.6	0.238	39
700	31.6	0.225	42
800	31.6	0.201	46

The recorded HRSEM images of the $BiFeO_3$ nanoparticles, sintered at 650 $^{\circ}C$ and 700$^{\circ}C$ have been depicted in Fig.3. From fig. it is observed that increase in the grain sizes becomes possible with an increase in the sintering temperature.

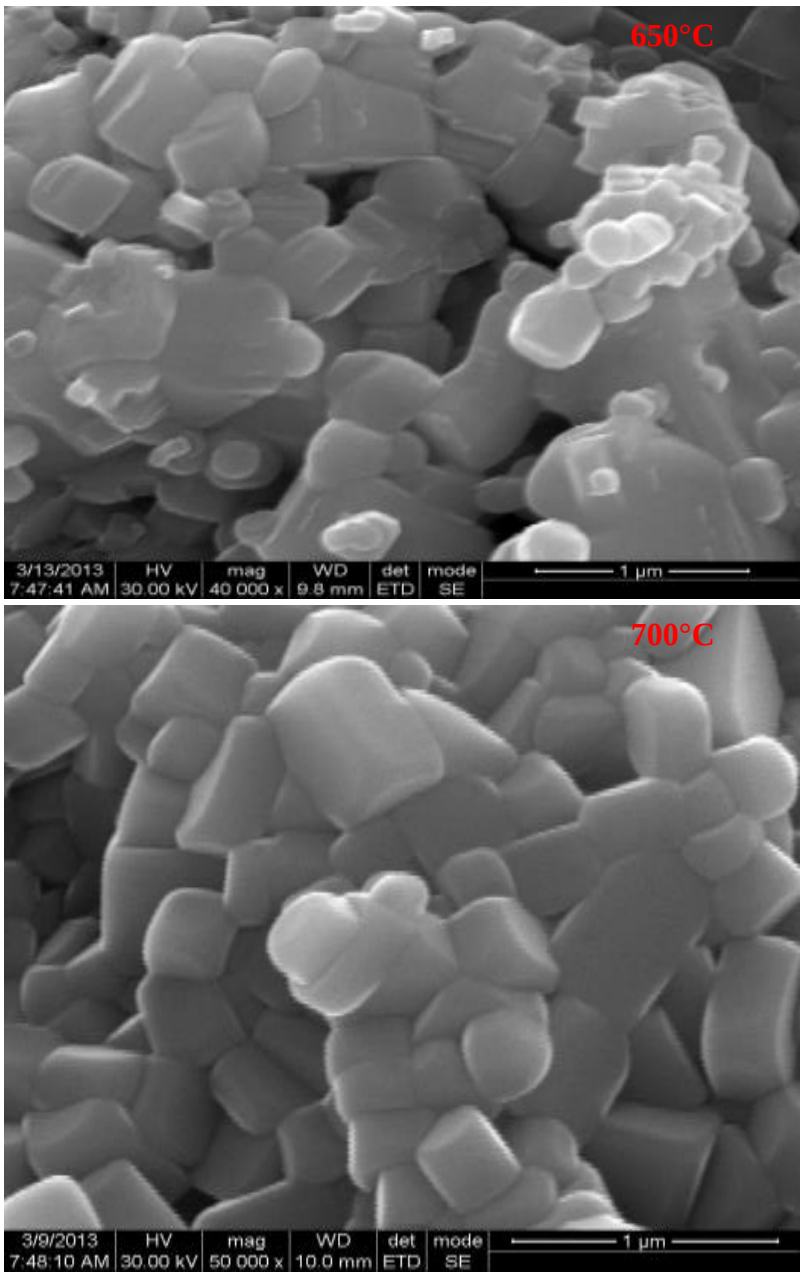

Fig.3. HR-SEM of $BiFeO_3$ nanoparticles sintered at different temperature

The sample sintered at 400 °C shows the porous and loosely packed grains microscopy with increasing the sintering temperature of sample at 500°C shows decrease in porosity with increase in the grain size and densely packed grain microscopy is observed. $BiFeO_3$ nanoparticles sintered at 500°C shows the grains which are in spherical shapes with average grain sizes in nm range. Upon increasing the temperature the grains sizes are continuously increasing [22-23] and appear to be like square shape at 600°C. However square shape grains increasing with sintered at 650 °C, 700 °C show grain boundaries are overlapped to each other and sample sintered at 800 °C(not shown), shows grain boundaries are completely overlapped with each other and densely packed microscopy.

From TG graph, at low temperature weith loss are occurring due to volatile particles, residual solvent, precipitation agent and others. These losses are purely depend method adopted for the preparation sample causes creation of dangling bond due to point defects and crystal dislocation causes induces the lattice strain in sample. During the sintering, the size and shape of the grain dependence on lattice strain plays a major role in nanostructure materials. Along with Gibbs Energy free energy at surface of the grain boundary causes diffusion of the atoms causes large in grain size.

The variation of magnetic properties of the $BiFeO_3$ nanoparticles with different sintered at 700 °C measuring M-H hysteresis loops as shown in Fig.4. $BiFeO_3$ exhibits Anti-ferromagnetism in bulk form and weak ferromagnetism in nanoparticles or thin films. This is due to the atomic and molecular hybridization causes anti parallel and parallel alignment of Fe^{3+}. During the atomic and molecular hybridization F^{3+} gets distorted based on john teller distortion causes small displacement polarization in [111] direction[24-27]. In addition to that, Due to the presence of the Dangling bond (an unsatisfied valence on an immobilized atom) in the sample due to unpaired electrons. These unpaired electrons of dangling bond contains of an electron contribute its own net magnetic moment causes change in net magmatic moment of the sample.

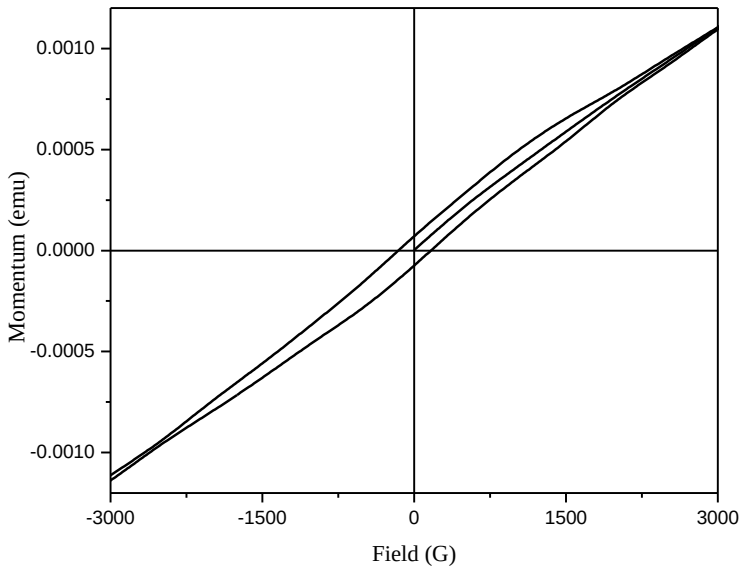

Fig.4. M-H hysteresis loops of $BiFeO_3$ nanoparticles sintered at 700 °C

Effect of grain size on electric polarization of $BiFeO_3$ nanoparticles with sintered at 700 $^{\circ}$C is measured and P-E hysteresis loops at room temperatures as show in Fig.5. $BiFeO_3$ nanoparticles exhibiting pontaneous polarization causes ferroelectric hysteresis loop at room temperature $BiFeO_3$. The reason for exhibiting spontaneous polarization of BiFeO3 nanoparticles is due to hybridization between active $6s^2$ lone pair of Bi^{+3} and oxygen 2p orbital. When Bismuth is Bi^{+3} state the empty 6p orbital of Bi^{+3} energy is closer to energy of oxygen 2p orbital, then hybridization takes place causes Bi^{+3} being displaced within its oxygen surroundings toward anion by breaking center of symmetry causes spontaneous polarization. And also due to small distortion of Fe^{+3} ion in octahedral symmetry with oxygen surrounding cause's spontaneous polarization also contributes to total polarization. Because this the reason $BiFeO_3$ exhibits large polarization. In present work, occurring of the oxygen defect randomly causes changes in hybridization causes changes in polarization direction causes decrease in net polarization value. Due to oxygen defect causes changes in distortion direction causes changes in polarization decreases. The ferroelectric polarization has two components. One component arises mainly from the non-collinear conical spin order associated with the spin-orbit coupling, which is thus magnetic field sensitive. The other is probably attributed to the Jahn-Teller distortion induced lattice symmetry breaking, occurring below the orbital ordering of Fe^{2+}. Furthermore, the coupled ferroelectric polarization and magnetization in response to magnetic field are observed. Due do change in the grain size remnant polarization also increased at 700° C is 0.033 μC/cm^2 respectively. Because, increasing the remnant the polarization (P_r) with increasing the grain size is due to high internal polarization, induced strain and electromechanical coupling. And decrease in coercivity with increasing in the sintering temperature indicates grain growth at higher sintering temperature [28].

An unclosed loops are observed which is due to the small leakage current is in the form of crystal defects (oxygen defects) observed. It is observed that the net polarization is decreased with presences of oxygen defects changes in orbital and molecular hybridization causes changes in polarization direction so that total polarization is decreased and also due to the presence of oxygen defect causes fluctuation of Fe^{+3} ions to Fe^{+2} state. In generally small leakage of maybe due to deviation from oxygen stoichiometry leads to valence fluctuation of Fe ions+3 to+2 state in $BiFeO_3$ [29]. The low leakage current and high (110) orientation contribute towards the improved ferroelectric behavior [30]. The $BiFeO_3$crystal structure belongs to the symmetry of a point group F = {3m}.The existence of a dielectric P-E hysteresis loop in dielectric materials implies that the substance possesses a spontaneous polarization and the value of the remanent polarization depends on the number of factors such as the dimensions of the specimen, the temperature, thermal and electrical properties of materials.

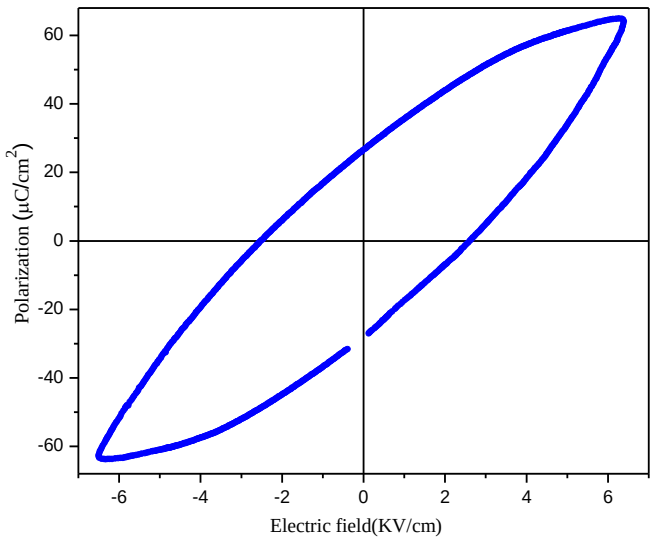

Fig.4. P-E hysteresis loopsof $BiFeO_3$ nanoparticles sintered at 700 $^{\circ}$C

Conclusion

In summary, it could be concluded that it has successfully synthesized BiFeO3 nanoparticles using a chemical co-precipitation method. From the TG profile, thermal decomposition process has been investigated. Energy change in the sample has been analyzed based on the existence of endothermic and exothermic peaks in DTA curve and its crystalline temperature has been found to be around 465◦C.From the analysis of TG-DTA results, valuable thermal parameters have been analyzed to understand the micro strain and its effect the sample. XRD analysis of the BiFeO3 sample shows the optimized sintered temperature is found to be at 700^{o}C. Both structural and morphological understanding of the samples has been made based on the measurements of SEM and analysised with thermodynamic parameters. From M-H graph Bismuth ferrite exhibiting anti-ferromagnetic properties at room temperature due to the other is probably attributed to the Jahn-Teller distortion induced lattice symmetry breaking, occurring below the orbital ordering of Fe2+.and remnant polarization also increased at 700° C is 0.033 μC/cm2 which is due to small distortion of Fe+3 ion in octahedral symmetry with oxygen surrounding cause's spontaneous polarization also contributes to total polarization. In addition to, A dangling bond contains an electron and can thus contribute its own net magnetic moment. Existence of the dangling bond contributes its own net magnetic moment and induces lattice strain that causes lattice distortion in sample casus large polarization. The effective magnetic and ferroelectric properties get enhanced due to dangling bonds along with coupling nature between ferroic orders in order to suit them for multifunctional devices applications.

References

[1] D. Sande, A. Agbelede, D. Rahmedov Crafting the magneonic and spintroinic response of Bifeo3 Films by epitaxial stain Nat. Mater. 12 (2013) 641-646.

[2] T. Zhao, A. Scholl, Electrical control of antiferromagnetic domains in multiferroic $BiFeO_3$ Films at room temperature. Nat. Mater. 5 (2006) 823-829.

[3] B. Kundvs, M. Viret, Light- induced size changes in $BiFeO_3$ crystals, Nat. Mater. 9 (2010) 803-805

[4] F. Changl, N. zhang, F. Yang, Effect of Cr substitution on the structure and electrical properties of $BiFeO_3$ ceramics, J. Phys. D: Appl. Phys. 40 (2007) 7799-7803.

[5] V. kothai, R. Ranjan, Synthesis of $BiFeO_3$ by carbonate precipitation, Bull. Mater. Sci., 2 (2012) 157-161.

[6] F. Gao, X. Chen, Visible-Light photocatalytic properties of weak magnetic $BiFeO_3$ nanoparticles, Adv. Matter., 19 (2007) 2889-2892.

[7] Hai-Feng Zhou, Hai-Ling Zhou, Enhanced magnetization and improved leakage in Er-doped $BiFeO_3$ nanoparticles, Phys. Stat. Solidi A 210 (2013) 809-813.

[8] T. Mashinol, S. Kimura, Synthesis of multiferroic BiFeO3 nanoparticles, J. Phys.: Conf. Series. 200 (2010) 072041.

[9] N. Andreev, N. Abramov , Fabrication and study of $GdMnO_3$ Multiferroic thin films Acta. Phys. Pol. A 117 (2010) 218-220.

[10] A. Pathak and P. Pramanik, Nano-particles of oxides through chemical method. INSA 67 (2001) 47–70

[11] A. Cziraki, Zs. Tonkovies, I. Geroes, and B. Fogarassy, Thermal stability of nanocrystalline nickel electrodeposits: differential scanning calorimetry, transmission electron microscopy and magnetic studies. Mat. Sci. Eng. A 179-180 (1994). 531–535.

[12] Y. L. Sun, S. F. Li, and D. H. Ding, Effect of ammonium oxalate or strontium carbonates on the burning rate characteristics of composite propellants. J. Therm. Anal. & Calorim. 86 (2006). 497–503.

[13] S. Ohta, T. K. Kosaka, and K. Sato, Study of Gd-doped cerium oxide by XRD, TG-DTA, impedance analysis and positron lifetime spectroscopy. J. Phys.: Conf. Series, 225 (2010) 012043.

[14] B. Jaya Prakasha, B. H. Rudramadevia & S. Buddhudua Analysis of Ferroelectric, Dielectric and Magnetic Properties of GdFeO3 Nanoparticles Ferroelectrics Letters Section, 41(2014)110–122.

[15] P. Muhammed Shafi and A. Chandra Bose Impact of crystalline defects and size on X-ray line broadening: A phenomenological approach for tetragonal SnO2 nanocrystals AIP Advances 5, (2015) 057137

[16] P.H. Suresha, Characterization of $BiFeO_3$ synthesized by microcontroller base theromgravimetric analyzer ,Indian J. Eng. Mater. Sci.19 (2012) 196-198.

[17] S. Iakovlev, C.-H. Solterbeck, Multiferroic $BiFeO_3$ thin films processed via chemical solution deposition:Structural and electrical characterization, J. Appl. Phys. 97 (2005) 094901

[18] J.K. Kim, S.S. Kim, Sol – Gel synthesis and properties of multiferroic $BiFeO_3$, Mater. Lett. 59 (2005) 4006-4009.

[19] H. Ke, W. Wang, Factors controlling pure-phase multiferroic BiFeO3 powders synthesized by chemical co-precipitation , J. Alloys Compd. 509 (2011) 2192-2197.

[20] S. Layek & H.C. Verma, Magnetic and dielectric properties of multiferroic $BiFeO_3$ nanoparticles synthesized by a novel citrate combustion method, Adv. Mater. Lett. 3 (2012) 533-538.

[21] D. Sande, A. Agbelede, D. Rahmedov Crafting the magneonic and spintroinic response of Bifeo3 Films by epitaxial stain Nat. Mater. 12 (2013) 641-646.

[22] H. Ke, W. Wang, Factors controlling pure-phase multiferroic BiFeO3 powders synthesized by chemical co-precipitation , J. Alloys Compd. 509 (2011) 2192-2197.

[23] S. Layek & H.C. Verma, Magnetic and dielectric properties of multiferroic $BiFeO_3$ nanoparticles synthesized by a novel citrate combustion method, Adv. Mater. Lett. 3 (2012) 533-538.

[24] Konstantin Komarov, Woojin Park, Accurate Spin–Orbit Coupling by Relativistic Mixed-Reference Spin-Flip-TDDFT. Journal of Chemical Theory and Computation *19* (2023) 953-964.
[25] Prachi Sharma, Andrew J. Jenkins, Exact-Two-Component Multiconfiguration Pair-Density Functional Theory. Journal of Chemical Theory and Computation *18* (2022) 2947-2954.
[26] Lixin Lu, Hang Hu, Andrew J. Jenkins, Component Relativistic Multireference Second-Order Perturbation Theory. Journal of Chemical Theory and Computation *18* (2022) 2983-2992.
[27] Yuji Noguchi, Takashi Goto, Masaru Miyayama, Ferroelectric distortion and electronic structure in $Bi4Ti_3O_{12}$, Journal of Electroceramics volume 21 (2008) 49–54

[28] D. Singh, K. kumara, Template synthesis and characterization of biologically active transition metal complexes comprising 14-membered tetraazamacrocyclic ligand.
J. Serb. Chem. Soc., 75 (2010) 217-228.

[29] K. Sigrist,DSC and X-ray measurement as method to detect lattice distortions
Thermochim. Acta., 311 (1998) 213-216.

[30] J. Li & T. Qiu, Synthesis of $SmAlO_3$ nanocrystalline powders by polymeric precursor method, Appl. Phys. A 104 (2011) 465-469.